Production of single-charmed baryons in a quark model approach

D. Iglesias-Ferrero,[1] D. R. Entem,[2,3,*] F. Fernández,[2,3,†] and P. G. Ortega[1,2,‡]

[1]*Departamento de Física Fundamental, Universidad de Salamanca, E-37008 Salamanca, Spain*
[2]*Instituto Universitario de Física Fundamental y Matemáticas (IUFFyM), Universidad de Salamanca, E-37008 Salamanca, Spain*
[3]*Grupo de Física Nuclear, Universidad de Salamanca, E-37008 Salamanca, Spain*

(Received 16 September 2022; accepted 2 November 2022; published 23 November 2022)

The production of single-charmed baryons $\Lambda_c^+\Lambda_c^-$, $\Lambda_c^+\Sigma_c^-$ + H.c., and $\Sigma_c^+\Sigma_c^-$ in $p\bar{p}$ collisions is studied in the framework of a constituent quark model that has satisfactorily described the $N\bar{N}$ system and the strangeness production $p\bar{p} \to \Lambda\bar{\Lambda}$, $\Lambda\bar{\Sigma}$, and $\Sigma\bar{\Sigma}$ processes. Predictions on the total cross sections are analyzed for different approaches to the underlying $n\bar{n} \to c\bar{c}$ process, mediated by one-gluon annihilation diagrams. The results indicate that the cross section is on the order of 1 nb between 10 and 14 GeV for $\Lambda_c^+\Lambda_c^-$ and $\Lambda_c^+\Sigma_c^-$ channels and around 0.01–0.1 nb for $\Sigma_c^+\Sigma_c^-$. These estimations can be relevant for their future search in facilities like PANDA.

DOI: 10.1103/PhysRevD.106.094027

I. INTRODUCTION

Charmed-hadron physics has been in the spotlight in the last years with the observation of many new excited states of charmed baryons and mesons, as well as exotic states with four or five minimum quark content (e.g., see a review in Refs. [1,2]). The construction of the PANDA experiment [3] at the Facility for Antiproton and Ion Research at GSI laboratory plans to push forward the research on charmed hadron spectroscopy and reactions with high-accuracy measurements [1].

Regarding charmed baryons, the program contains not only a study of the spectroscopy, but also in-medium effects, charm-anticharm mixing, the search for CP violation or studies of precise measurements of Λ_c decays. A required previous step is the estimation of charm production cross sections in $p\bar{p}$ collisions. Indeed, charm production processes in proton-antiproton reactions are important to test the mechanisms of charm quark pair creation, which is in the regime of nonperturbative QCD. In particular, increasing interest is being given to the exclusive production reactions such as $p\bar{p} \to \Lambda_c^+\Lambda_c^-$.

This process is the prototype reaction to analyze the underlying process of charm quark pair creation in baryons. The process recalls the hyperon production reaction $p\bar{p} \to \Lambda\bar{\Lambda}$. Traditionally, two different pictures have been used to describe the strangeness production. One of them is based on the t-channel meson exchange [4], whereas the second works at the quark level being the strangeness created by $q\bar{q}$ annihilation and subsequent $s\bar{s}$ creation by s-channel gluon exchanges [5].

Both models can be extended to the $Y_c\bar{Y}_c$ production. The extension of the meson-exchange model to the charm sector is based on $SU(4)$ flavor symmetry. Accordingly, the elementary charm production process is described by t-channel D and D^* meson exchanges. Such a model has been applied to the charm production in Ref. [6]. However, up until now, the quark model has not been extended to the charm production.

Other models, including quark-gluon string models [7,8], effective Lagrangian models [9–11], and perturbative QCD calculation within the handbag approach [12], have been used to describe the charm production, with a disparity of predictions ranging over several orders of magnitude.

One characteristic feature of the $Y_c\bar{Y}_c$ production is that different final channels are produced via selected isospin channels: the $\Lambda_c^+\bar{\Lambda}_c^-$ is produced via the isospin singlet ($I = 0$) channel, whereas the $\Lambda_c^+\bar{\Sigma}_c^-$ + H.c. goes through the isospin triplet ($I = 1$). This fact can be used to differentiate models that involve different physics. In the conventional meson-exchange picture, the charm production transition interaction is weaker than the $Y\bar{Y}$ production mediated by kaon exchanges, but it predicts larger cross sections than alternative models based on s-channel exchanges. However, this latter model will show a dominance of spin-triplet channels, since the spin of the Λ_c is

*entem@usal.es
†fdz@usal.es
‡pgortega@usal.es

entirely carried by the c quark, so a triplet $c\bar{c}$, produced by an effective vector as the gluon, guarantees a triplet $\Lambda_c\bar{\Lambda}_c$ final state.

Unfortunately, unlike the hyperon-antihyperon reactions, the charmed baryon production lacks experimental data, so there is no way to discriminate among models. Nevertheless, the theoretical calculations allow one to predict the order of magnitude of the observables, which can be of help for the future experimental search.

In view of the experimental and theoretical interests in such reactions, in this paper we analyze the $Y_c\bar{Y}_c$ production reaction using a widely used constituent quark model [13,14]. The model has been extensively used to describe hadronic spectroscopy and reactions [15–19], as well as the $p\bar{p}$ cross section and positronium level shifts [20] and the analog strangeness process of proton-antiproton to hyperon-antihyperon [5,21]. Besides the one-gluon exchange [22], the constituent quark model encodes constituent masses, emerging as a dynamical mass generated by the spontaneous breaking of the $SU(3)_L \otimes SU(3)_R$ symmetry of the QCD Lagrangian. Hence, as a consequence of the Nambu-Goldstone theorem, eight massless bosons identified with the members of the pseudoscalar octet $\{\pi, K, \eta\}$, corresponding with the eight broken generators, are expected to be exchanged between the massive quarks. Thus, this model shares features of meson-exchange and quark-gluon models in a unified framework.

In this approach, the $n\bar{n} \to c\bar{c}$ transition is described via a gluon annihilation diagram, building the hadronic $p\bar{p} \to Y_c\bar{Y}_c$ transition interactions by means of the resonating group method, which folds the quark level interaction with the wave functions of the baryons under play. This feature implies that the $\Lambda_c^+\Lambda_c^-$ production will occur in a pure spin-triplet state, the spin-singlet channels being completely suppressed. Nambu-Goldstone boson exchanges do not affect the transition potential, but constrain the initial and final state interactions.

The paper is organized as follows: In Sec. II, we describe the details of the constituent quark model and the calculation of the cross section in a coupled-channels approach. In Sec. III, we present the results and a comparison with other theoretical estimations, and in Sec. IV we give a short summary.

II. THE MODEL

The predictions for the production of Λ_c/Σ_c are based on previous analyses of strangeness production in proton-antiproton collisions [5,21]. Such calculations, and those in the present study, were done in the framework of the constituent quark model described in Ref. [20] for the $N\bar{N}$ system. All the parameters of the model have been constrained from previous calculations of hadron phenomenology, so in that sense the results are parameter-free.

Based on Diakonov's picture of the QCD vacuum as a dilute instanton liquid [23], the model assumes that the quark acquires a dynamical mass due to the interaction with fermionic zero modes of individual instantons. The momentum-dependent mass vanishes for large momenta and acts as a natural cutoff of the theory. This scenario can be modeled with the chiral invariant simple Lagrangian [23]

$$\mathcal{L} = \bar{\psi}(i\gamma^\mu\partial_\mu - MU^{\gamma_5})\psi, \tag{1}$$

where $U^{\gamma_5} = \exp(i\phi^a\lambda^a\gamma_5/f_\pi)$, where ϕ^a denotes the pseudoscalar fields $(\vec{\pi}, K_i, \eta_8)$ with $i = (1, \ldots, 4)$, λ^a being the $SU(3)$ flavor matrices, and with M as the constituent quark mass. The momentum dependence of the constituent quark mass can be derived from the theory, though a simpler parametrization can be obtained as $M(q^2) = m_q F(q^2)$, where $m_q \sim 300$ MeV and

$$F(q^2) = \sqrt{\frac{\Lambda_\chi^2}{\Lambda_\chi^2 + q^2}}, \tag{2}$$

with Λ_χ being a cutoff that fixes the chiral symmetry-breaking scale.

Expanding the Nambu-Goldstone boson field matrix U^{γ^5} from Eq. (1), we have

$$U^{\gamma_5} = 1 + \frac{i}{f_\pi}\gamma_5\lambda^a\phi^a - \frac{1}{2f_\pi^2}\phi^a\phi^a + \ldots, \tag{3}$$

where we can identify the constituent quark mass contribution in the first term. Further terms give rise to quark-quark interactions mediated by boson exchanges. Specifically, the second term represents the $\phi^a = \{\vec{\pi}, K_i, \eta_8\}$ one-boson exchange, with $i = (1, \ldots, 4)$, whereas the third term illustrates a two-boson exchange, whose main contribution can be modeled as a scalar σ exchange.

Such boson exchanges, detailed in Refs. [5,13], allow one to describe the $N\bar{N}$ and $Y_c\bar{Y}_c$ self-interactions, constrained by the light-quark potentials. The basic $q\bar{q}$ potentials for such systems are

$$\begin{aligned}
V^\pi_{q\bar{q}}(\vec{q}) &= \frac{1}{(2\pi)^3}\frac{g_{ch}^2}{4m_q^2}\frac{\Lambda_\pi^2}{\Lambda_\pi^2 + q^2}\frac{(\vec{\sigma}_i\cdot\vec{q})(\vec{\sigma}_j\cdot\vec{q})}{m_\pi^2 + q^2}(\vec{\tau}_i\cdot\vec{\tau}_j),\\
V^\eta_{q\bar{q}} &= -\frac{1}{(2\pi)^3}\frac{g_{ch}^2}{4m_q^2}\frac{\Lambda_\eta^2}{\Lambda_\eta^2 + q^2}\frac{(\vec{\sigma}_i\cdot\vec{q})(\vec{\sigma}_j\cdot\vec{q})}{m_\eta^2 + q^2}\\
&\quad\times(\cos\theta_P\lambda_i^8\lambda_j^{8\dagger} - \sin\theta_P),\\
V^\sigma_{q\bar{q}}(\vec{q}) &= -\frac{g_{ch}^2}{(2\pi)^3}\frac{\Lambda_\sigma^2}{\Lambda_\sigma^2 + q^2}\frac{1}{m_\sigma^2 + q^2},
\end{aligned} \tag{4}$$

diagrammatically represented in Fig. 1(a). The parameters of the model are presented in Table I. The chiral coupling constant g_{ch} is determined from the πNN coupling constant, through the relation

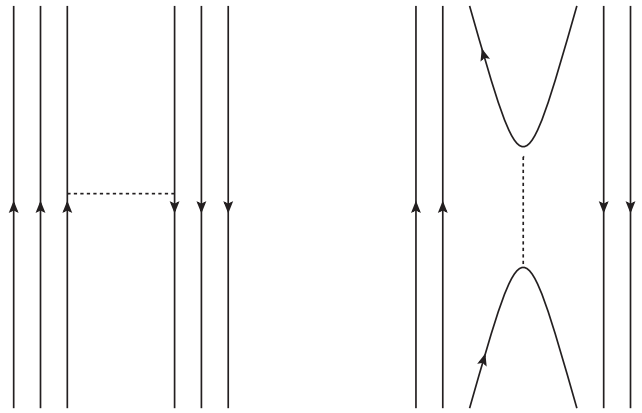

(a) (b)

FIG. 1. Possible diagrams for the $N\bar{N}$ and $\Lambda_c\bar{\Lambda}_c$ interactions: (a) Nambu-Goldstone boson exchange mechanisms and (b) Annihilation mechanisms.

$$\frac{g_{ch}^2}{4\pi} = \left(\frac{3}{5}\right)^2 \frac{g_{\pi NN}^2}{4\pi}\frac{m_q^2}{m_N^2},$$

with m_q as the mass of the light $\{u, d\}$ quark [13].

Nevertheless, the charm production $n\bar{n} \to c\bar{c}$, with $n = \{u, d\}$, is beyond the chiral symmetry-breaking scale. Hence, within our constituent quark model, such production mechanism is not mediated by Nambu-Goldstone boson exchanges, but it is governed by QCD perturbative effects, which are taken into account through the one-gluon-exchange term

$$\mathcal{L}_{gqq} = i\sqrt{4\pi\alpha_s}\bar{\psi}\gamma_\mu G_c^\mu \lambda^c \psi, \tag{5}$$

λ^c being the $SU(3)$ color matrices and G_c^μ is the gluon field. The strong coupling constant α_s has a scale dependence that allows one to consistently describe light, strange, and heavy mesons, whose explicit expression is

$$\alpha_s(\mu) = \frac{\alpha_0}{\ln(\frac{\mu^2+\mu_0^2}{\Lambda_0^2})}, \tag{6}$$

where μ is the reduced mass of the $q\bar{q}$ system and α_0, μ_0, and Λ_0 are parameters of the model (see Table I).

Since quark-antiquark exchanges are not allowed in $N\bar{N}$ or $Y_c\bar{Y}_c$ systems, the $N\bar{N}$ ($Y_c\bar{Y}_c$) interaction from one-gluon exchange (OGE) only emerges as annihilation diagrams, that is, in momentum representation [20,24],

$$V_{q\bar{q}}^{A,\mathrm{OGE}}(\vec{q}) = \frac{\alpha_s}{8\pi^2 m_{ij}}\left(\frac{4}{9} - \frac{1}{12}\vec{\lambda}_1\cdot\vec{\lambda}_2\right) \times \left(\frac{3}{2} + \frac{1}{2}\vec{\sigma}_1\cdot\vec{\sigma}_2\right)\left(\frac{1}{2} - \frac{1}{2}\vec{\tau}_1\cdot\vec{\tau}_2\right), \tag{7}$$

where m_{ij} is the product of the masses of the interacting quarks. For the $N\bar{N} \to Y_c\bar{Y}_c$, those are $m_{ij} = m_n^2$, with m_n as the mass of the light quarks $\{u, d\}$. However, this choice may overestimate the contribution of the gluon annihilation interaction for an $n\bar{n} \to c\bar{c}$ process, whose energy is much larger than m_n. For that reason, we will compare the results with $m_{ij} = m_n^2$, which will be dubbed "model (a)" from now on, with an averaged quark mass $m_{ij} = \overline{m_\Lambda}^2$, where $\overline{m_\Lambda} = \frac{1}{3}(2m_n + m_c)$, which is dubbed "model (b)." The value of the $\alpha_s(\mu)$ from Eq. (6) will be scaled accordingly.

TABLE I. Quark model parameters.

Quark masses	m_n (MeV)	313
	m_c (MeV)	1763
Nambu-Goldstone bosons	m_π (MeV)	138
	m_σ (MeV)	693
	m_η (MeV)	546.5
	$\Lambda_\pi = \Lambda_\sigma$ (MeV)	848.33
	Λ_η (MeV)	1025.96
	$g_{ch}^2/(4\pi)$	0.54
	θ_P (°)	−15
OGE	α_0	2.118
	μ_0 (MeV)	36.976
	Λ_0 (fm^{-1})	0.113

In the $q\bar{q}$ system, there are also annihilation contributions from Nambu-Goldstone bosons [Fig. 1(b)] in the $N\bar{N} \to N\bar{N}$ and $Y_c\bar{Y}_c \to Y_c\bar{Y}_c$ reactions. In our model, the real part of this potential can be obtained with a Fierz transformation of Eq. (4). Explicit expressions can be found in Ref. [5].

The last ingredient of our constituent quark model is confinement, a nonperturbative effect that prevents having colored hadrons. This potential contributes neither to the $N\bar{N}$ nor to the $Y_c\bar{Y}_c$ interactions, but allows one to describe hadron spectroscopy and prevents the baryon collapse under the interactions described above.

Finally, in addition to the interaction in the elastic channels, both $p\bar{p}$ and $Y_c\bar{Y}_c$ annihilate into mesons, processes that are very complex to describe. These contributions are usually parametrized in terms of optical potentials. In order to evaluate the model predictions of the total cross section near the $Y_c\bar{Y}_c$ threshold, we will take the $Y_c\bar{Y}_c$ optical potential to be zero, as it is not expected to have a large influence in this energy region. For the $N\bar{N}$ optical potential, with the aim of simplifying the description of the processes, we do not include spin-orbit or tensor pieces. Thus, we take the form

$$V_{\mathrm{Opt}} = (V_r + i\cdot W_i)e^{-\frac{d^2}{2}q^2}, \tag{8}$$

where the d, V_r, and W_i parameters are fitted to the available total, elastic, and inelastic $p\bar{p} \to p\bar{p}$ cross sections up to $p_{\mathrm{lab}} = 14$ GeV (see Fig. 2), obtaining the values $d = 0.509$ fm, $V_r = -0.184$ GeV^{-2}, and $W_i = -2.041$ GeV^{-2}. We consider a 10% error in such parameters, though the

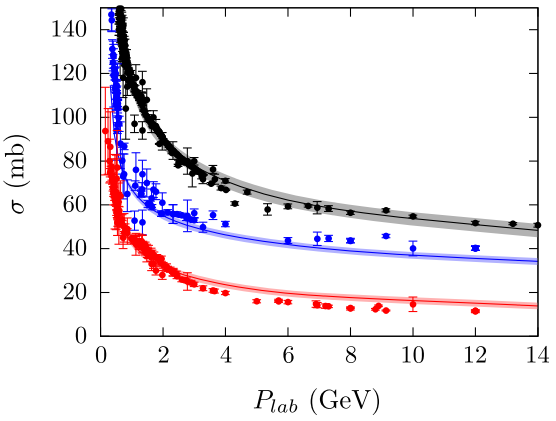

FIG. 2. Total (black line), inelastic (blue) and elastic (red) $p\bar{p} \to p\bar{p}$ cross sections. Experimental data from Refs. [26]. The shadowed bands around the lines show the sensitivity of the cross sections when the value of the V_r and W_i parameters are varied a 10%.

impact of such uncertainty is negligible in the full $p\bar{p} \to Y_c\bar{Y}_c$ reaction.

The baryon-antibaryon interaction is obtained from the microscopic description using the resonating group method (RGM), obtaining an effective cluster-cluster interaction from the underlying quark-quark dynamics, where the wave functions of the baryons act as natural cutoffs of the $q\bar{q}$ potentials.

The wave function for the baryon (antibaryon) states is

$$\psi_B = \phi_B(\vec{p}_\lambda, \vec{p}_\rho)\chi_B\xi_c[1^3], \tag{9}$$

where χ_B is the spin-isospin wave function, ξ_c is the color wave function, and ϕ_B is the orbital wave function, with $\vec{p}_\lambda$ and $\vec{p}_\rho$ the momenta of the λ and ρ modes. For the N ($\bar{N}$) wave function, a good description can be achieved with a Gaussian with range $b = 0.518$ fm [20].

To solve the three-body Schrödinger equation, we use the Gaussian expansion method [25]. In this method, the radial wave function is expanded in terms of basis functions whose parameters are in geometrical progression,

$$\phi_B^{LM} = \sum_{n_\lambda, n_\rho}^{n_{\max}} C_{n_\lambda,n_\rho}[\phi_{n_\lambda,\ell_\lambda}(\vec{p}_\lambda)\phi_{n_\rho,\ell_\rho}(\vec{p}_\rho)]_{LM}, \tag{10}$$

where L is the total angular momentum, satisfying $L = \ell_\lambda \oplus \ell_\rho$, and C_{n_ρ,n_λ} are the coefficients of the base expansion. The ϕ functions are defined as

$$\phi_{n,\ell m}(\vec{p}) = N_{n\ell} p^\ell e^{-\frac{1}{4\eta_n}p^2} Y_{\ell m}(\hat{p}), \tag{11}$$

with $N_{n\ell}$ the normalization of the Gaussian wave functions such that $\langle\phi_{n\ell}|\phi_{n\ell}\rangle = 1$.

The coefficients C_{n_λ,n_ρ} and the eigenenergies of the baryons are determined from the Rayleigh-Ritz variational principle,

$$\sum_{n=1}^{n_{\max}} [(T^{\alpha'}_{n'n} - EN^{\alpha'}_{n'n})C^{\alpha'}_n + \sum_\alpha V^{\alpha'\alpha}_{n'n}C^\alpha_n] = 0, \tag{12}$$

with $n = \{n_\lambda, n_\rho\}$, $T^{\alpha'}_{n'n}$ and $N^{\alpha'}_{n'n}$ as the kinetic and normalization operators, which are diagonal, and $V^{\alpha'\alpha}_{n'n}$ as the underlying $q\bar{q}$ interaction from the constituent quark model detailed above.

Then, the scattering problem is solved using the coupled-channel Lippmann-Schwinger equation,

$$T^{\beta'}_\beta(z; p', p) = V^{\beta'}_\beta(p', p) + \sum_{\beta''}\int dp'' p''^2 V^{\beta'}_{\beta''}(p', p'') \times \frac{1}{z - E_{\beta''}(p'')} T^{\beta''}_\beta(z; p'', p), \tag{13}$$

where β represents the set of quantum numbers necessary to determine a partial wave $B\bar{B}JLST$, $V^{\beta'}_\beta(p', p)$ is the RGM potential, and $E_{\beta''}(p'')$ is the energy for the momentum p'' referred to as the lower threshold.

The RGM potentials are proportional to the underlying qq interactions, modified with a form factor that encodes the baryon-antibaryon structure. As an illustration, the RGM potentials for the $N\bar{N} \to Y_c\bar{Y}_c$ can be written as

$${}^{\rm RGM}V_{N\bar{N}\to Y_c\bar{Y}_c}(p', p) = \mathcal{F}(\vec{p}', \vec{p})^2 V_{n\bar{n}\to c\bar{c}}(\vec{p}' - \vec{p}), \tag{14}$$

where $V_{n\bar{n}\to c\bar{c}}$ is the underlying constituent quark model potential and $\mathcal{F}$ is the $N \to Y_c$ ($\bar{N} \to \bar{Y}_c$) form factor,

$$\mathcal{F}(\vec{p}', \vec{p}) = \sqrt{8}\sum_{n_\lambda, n'_\lambda}^{n_{\max}} C_{n_\lambda} C_{n'_\lambda} \frac{(\eta_{n_\lambda}\eta_{n'_\lambda})^{3/4}}{(\eta_{n_\lambda} + \eta_{n'_\lambda})^{3/2}} e^{-\frac{Q^2}{4(\eta_{n_\lambda} + \eta_{n'_\lambda})}}, \tag{15}$$

with $Q = (\frac{2m_n}{m_c+2m_n}\vec{p}' - \frac{2}{3}\vec{p})$ as the transferred momentum. Here, C_{n_λ} ($C_{n'_\lambda}$) and η_{n_λ} ($\eta_{n'_\lambda}$) are, respectively, the λ-mode coefficients and ranges of the N (Y_c) wave function of Eq. (11).[1]

A full coupled-channels study is performed. The interactions of the diagonal channels, $p\bar{p} \to p\bar{p}$ and $Y_c\bar{Y}_c \to Y_c\bar{Y}_c$, contribute to the initial and final state interactions. For the $p\bar{p}$ channel, the interactions included are the exchange of π, σ, and η mesons in the t channel and the pion and gluon annihilation in the s channel. The $Y_c\bar{Y}_c$ interaction is due to the π, σ, and η exchanges in the t channel and the gluon, π, and η exchanges in the s channel. The nondiagonal interaction $p\bar{p} \to Y_c\bar{Y}_c$ is solely due to gluon annihilation in the s channel.

[1]In this example, the λ mode is taken as the coordinate between the heavy quark c and the light pair nn. With this choice, the ρ mode (coordinate between the two light n quarks) can be integrated out in Eq. (15).

Before presenting the results, note here that our constituent quark model merges traditional boson-exchange and annihilation pictures in a unified framework. The mesons are generated as Nambu-Goldstone bosons of the spontaneous chiral symmetry breaking and gluons as perturbative contributions from QCD. For the case of $\Lambda\bar{\Lambda}$ this mixture allowed for a description of the total cross section and observables without any fine-tuning of the model parameters. In the case of single-charmed baryons, the boson-exchange diagrams do not contribute to the production mechanism, so the total cross section will be much smaller than other models based on meson exchanges.

III. RESULTS

The description of the $p\bar{p} \to p\bar{p}$ cross section is a necessary step before describing the single-charmed baryon production. Previous works [5,20] focused on the low-energy region of the $N\bar{N}$ system, so we do not expect the parameters of the optical potential considered in those works to hold at the $\Lambda_c^+\Lambda_c^-$ threshold. For the large production energies of the $Y_c\bar{Y}_c$ pairs, the optical potential dominates the total, elastic, and inelastic $N\bar{N}$ cross sections. In order to describe the broad experimental data, gathered by Ref. [26], we have considered a simple optical potential of the form of Eq. (8). The parameters are fitted to the $p\bar{p} \to p\bar{p}$ total, elastic, and inelastic cross sections. A good description of the total, elastic, and inelastic cross sections is achieved, as we show in Fig. 2, which validates the model in the relevant energy range. In this figure, a 10% variation of the V_r and W_i parameters of Eq. (8) is included in order to evaluate the sensitivity of the $p\bar{p} \to p\bar{p}$ cross sections. Albeit, the impact of such variation in the $p\bar{p} \to Y_c\bar{Y}_c$ cross section was found to be negligible.

Because of the lack of experimental data for the $\Lambda_c^+\Lambda_c^-$, $\Lambda_c^+\Sigma_c^-$, or $\Sigma_c^+\Sigma_c^-$ channels, it is difficult to determine the optical potential parameters for the final channels. For the strangeness production [21], the $p\bar{p} \to \Lambda\bar{\Lambda}$ total cross section was used to fit these parameters but, in this case, there is no available experimental data for the $p\bar{p} \to Y_c\bar{Y}_c$. For this reason, no optical potential will be considered for the final channels. Nevertheless, we have tested the sensitivity of the $p\bar{p} \to Y_c\bar{Y}_c$ total cross section to the optical potential of the final channel using the parametrization for the $\Lambda\bar{\Lambda}$, $\Lambda\bar{\Sigma} + \text{H.c.}$, and $\Sigma\bar{\Sigma}$ channels used in Ref. [21], comparing them with the results without the optical potential, and we found that the effect of the optical potential is small in the region close to threshold.

We show in Fig. 3 the results for the $p\bar{p} \to \Lambda_c^+\Lambda_c^-$ total cross section predicted in this work, compared with other theoretical estimations. We show the total cross section for the two models discussed in Sec. II, which consider different assumptions for the one-gluon annihilation process $n\bar{n} \to c\bar{c}$. The so-called model (a), which takes

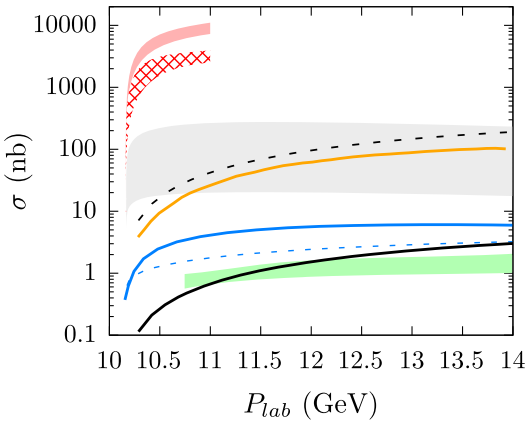

FIG. 3. Total cross section for $p\bar{p} \to \Lambda_c^+\Lambda_c^-$ for model (a) (black dashed line) and model (b) (black solid line), compared with other studies: The meson-exchange frameworks of Ref. [6] (where solid red band for meson exchange and square red band for quark-gluon transition potential) and Ref. [11] (with Regge approach in blue solid line and effective Lagrangian in blue dashed line), the QGS models of Ref. [7] (gray band) and Ref. [8] (orange line), and the perturbative QCD calculation of Ref. [12] (green band).

$m_{ij} = m_n^2$ in Eq. (7), is almost 2 orders of magnitude larger than model (b), which takes $m_{ij} = \bar{m_\Lambda}^2$, where $\bar{m_\Lambda}$ is the averaged constituent mass of the Λ_c baryon, that is, $\bar{m_\Lambda} = \frac{1}{3}(2m_n + m_c)$. That indicates the sensitivity of the results to the specific quark propagator in the transition potential. Model (a) is of the same order of magnitude as other theoretical approaches, such as the quark-gluon string (QGS) models of Refs. [7,8]. On the other hand, model (b), which considers a quark propagator more in line with the energy region of the charmed baryon thresholds, predicts a similar cross section as the perturbative QCD calculation of Ref. [12]. In our model, the $n\bar{n} \to c\bar{c}$ transition is beyond the chiral symmetry-breaking scale, so no meson exchange is allowed, which explains why the total cross section is much smaller than the estimates from D and D^* exchange frameworks of Ref. [6]. The latter work also considered a $^3S_1$ transition interaction mediated by a gluon, but it is likely that the quark-gluon coupling strength was overestimated. Recent studies of Ref. [11] using boson exchanges mediated by the $D + D^*$ mesons with a Regge approach and effective Lagrangian show smaller cross sections, comparable with our calculations for model (b).

The $p\bar{p} \to \Lambda_c^+\Sigma_c^- + \text{H.c.}$, Fig. 4, shows a similar pattern as the $p\bar{p} \to \Lambda_c^+\Lambda_c^-$. Interestingly, in this case the total cross section of model (a) is close to the quark model predictions of Haidenbauer and Krein [6] and the QGS of Khodjamirian *et al.* [7]. Model (b), on the contrary, is almost 2 orders of magnitude below, closer to the results of Ref. [11]. Equivalent conclusions can be obtained for the $p\bar{p} \to \Sigma_c^+\Sigma_c^-$, shown in Fig. 5, but in this case the total cross

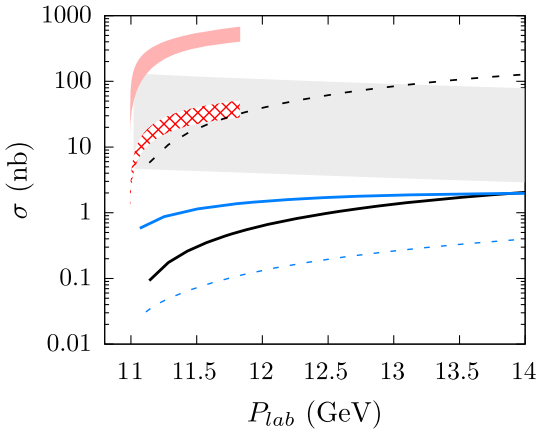

FIG. 4. Total cross section for $p\bar{p} \to \Lambda_c^+\Sigma_c^- + \text{H.c.}$ Same legend as in Fig. 3.

section is 1 order of magnitude smaller than those of $p\bar{p} \to \Lambda_c^+\Lambda_c^-$ and $\Lambda_c^+\Sigma_c^- + \text{H.c.}$ for both models.

In Fig. 6 we show the contribution of each partial wave to the total cross section, in percentage, of $p\bar{p} \to \Lambda_c^+\Lambda_c^-$ and $p\bar{p} \to \Lambda_c^+\Sigma_c^- + \text{H.c.}$ at $\sqrt{s} = 12$ GeV, depending on their total momentum J. The contributions are split in two types: the spin-singlet (${}^1L_J \to {}^1L_J$, with $L = J$) and spin-triplet (${}^3L_J \to {}^3L_J$, with $L = J-1,\ J, J+1$) transitions. We should emphasize that the one-gluon annihilation potential is purely central, so the orbital momentum is always conserved and, thus, the nondiagonal ${}^3(J \pm 1)_J \to {}^3(J \mp 1)_J$ transition interactions are zero. For both cases, it is interesting to notice a predominance of partial waves with large J, with a maximum around $J = 12$–13. Such maximum is due to the enhancement of large J partial waves in the initial $N\bar{N}$ channel for the $Y_c\bar{Y}_c$ production energy region. The S wave is practically zero, because the S wave of the initial $N\bar{N}$ is negligible for the energy range under study.

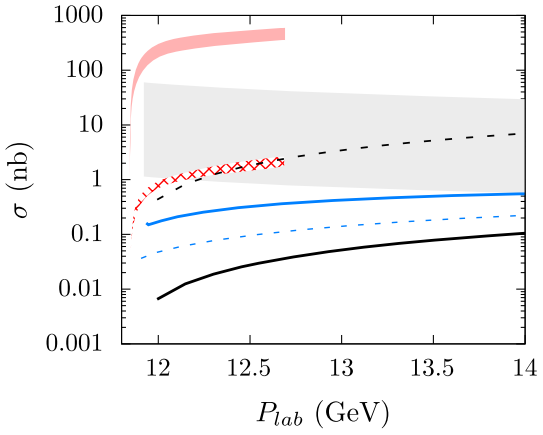

FIG. 5. Total cross section for $p\bar{p} \to \Sigma_c^+\Sigma_c^-$. Same legend as in Fig. 3.

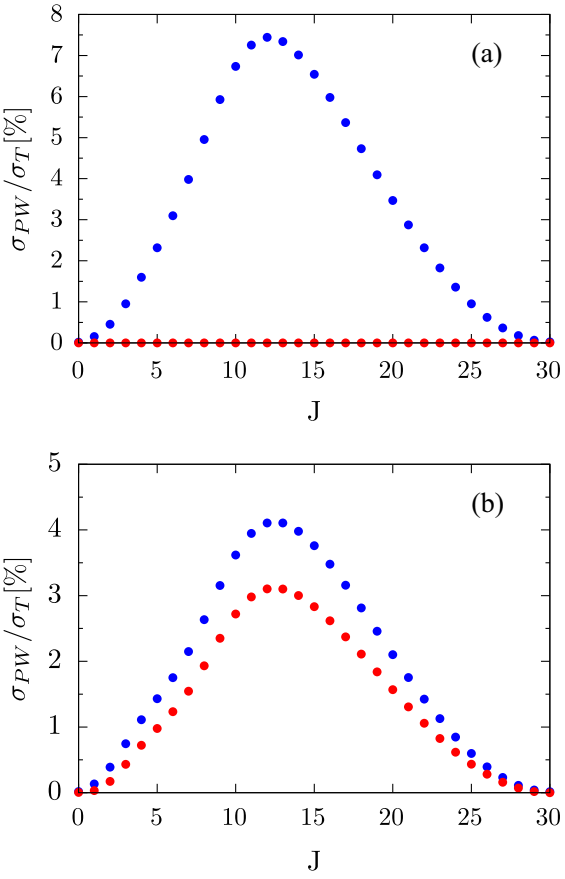

FIG. 6. Contribution of different partial waves, in percentage, to the total cross section of (a) $p\bar{p} \to \Lambda_c^+\Lambda_c^-$ and (b) $p\bar{p} \to \Lambda_c^+\Sigma_c^- + \text{H.c.}$ at $\sqrt{s} = 12$ GeV. Blue dots represent the spin-triplet and red dots the spin-singlet transitions.

For the isospin-0 $p\bar{p} \to \Lambda_c^+\Lambda_c^-$ process [Fig. 6(a)] the one-gluon annihilation potential is zero for the spin-singlet channel, so the only contributions to the cross section are the spin-triplet channels. That is reasonable as the total spin of the Λ_c is carried by the charm quark c and the production of the $c\bar{c}$ is mediated by a vector field, that is, the gluon. The isospin-1 $p\bar{p} \to \Lambda_c^+\Sigma_c^- + \text{H.c.}$ process shows a similar pattern for the spin-triplet channels but, in this case, we have contribution from both spin-singlet and -triplet channels, with a ratio in the OGE coefficients of Eq. (7) of $C_{S=0}/C_{S=1} = 3/2$. The partial wave decomposition for the $p\bar{p} \to \Sigma_c^+\Sigma_c^-$ follows the same pattern, with a maximum around $J \sim 12$, having contributions from both spin-singlet and -triplet components, as well as also isospin-0 and -1 channels.

This feature produces an abrupt increase of the cross section in the region close to threshold; a behavior that was also measured in the strangeness production $p\bar{p} \to \Lambda\bar{\Lambda}$.

IV. SUMMARY

In this work we have performed a coupled-channels calculation of the $p\bar{p} \to \Lambda_c^+\Lambda_c^-$, $\Lambda_c^+\Sigma_c^- + \text{H.c.}$, and $\Sigma_c^+\Sigma_c^-$

within a constituent quark model that properly describes the $N\bar{N}$ system [20] and the production of strangeness in $p\bar{p}$ collisions [5,21]. We have compared the results with other theoretical models, showing that our approach predicts a total cross section consistent with previous studies, in the range of 0.1–10 nb for the $\Lambda_c^+\Lambda_c^-$ final channel close to threshold, depending on the assumptions taken in the gluon annihilation transition potential. Considering the energy ranges involved in the reaction, the so-called model (b) seems more realistic, which would lead to a cross section on the order of 1 nb, similar to perturbative QCD estimations [12].

Thus, this study suggests that the experimental detection of the process of charm production under study can be challenging, but perfectly reachable at PANDA considering the planned luminosity on the order of 10^{32} cm^{-2} s^{-1}, which could provide valuable information on the underlying $n\bar{n} \to c\bar{c}$ production mechanisms.

ACKNOWLEDGMENTS

This work has been partially funded by Ministerio de Ciencia, Innovación y Universidades under Contract No. PID2019–105439 GB-C22/AEI/10.13039/501100011033 and by the EU Horizon 2020 research and innovation program, STRONG-2020 project, under Grant Agreement No. 824093.

[1] U. Wiedner, Future prospects for hadron physics at PANDA, Prog. Part. Nucl. Phys. **66**, 477 (2011).
[2] F.-K. Guo, C. Hanhart, U.-G. Meißner, Q. Wang, Q. Zhao, and B.-S. Zou, Hadronic molecules, Rev. Mod. Phys. **90**, 015004 (2018).
[3] M. F. M. Lutz *et al.* (PANDA Collaboration), Physics Performance Report for PANDA: Strong Interaction Studies with Antiprotons, arXiv:0903.3905.
[4] J. Haidenbauer, T. Hippchen, K. Holinde, B. Holzenkamp, V. Mull, and J. Speth, Reaction $p\bar{p} \to \Lambda\bar{\Lambda}$ in the meson-exchange picture, Phys. Rev. C **45**, 931 (1992).
[5] P. G. Ortega, D. R. Entem, and F. Fernandez, $p\bar{p} \to \Lambda\bar{\Lambda}$ depolarization and spin transfer in a constituent quark model, Phys. Lett. B **696**, 352 (2011).
[6] J. Haidenbauer and G. Krein, Production of charmed baryons in $\bar{p}p$ collisions close to their thresholds, Phys. Rev. D **95**, 014017 (2017).
[7] A. Khodjamirian, C. Klein, T. Mannel, and Y. M. Wang, How much charm can PANDA produce?, Eur. Phys. J. A **48**, 31 (2012).
[8] A. B. Kaidalov and P. E. Volkovitsky, Binary reactions in $\bar{p}p$ collisions at intermediate-energies, Z. Phys. C **63**, 517 (1994).
[9] Q.-Y. Lin and X. Liu, Production of charmed baryon $\Lambda c(2860)$ via low energy antiproton-proton interaction, Phys. Rev. D **105**, 014035 (2022).
[10] R. Shyam, Charmed-baryon production in antiproton-proton collisions within an effective Lagrangian model, Phys. Rev. D **96**, 116019 (2017).
[11] T. Sangkhakrit, S.-I. Shim, Y. Yan, and A. Hosaka, Charmed baryon pair production in proton-antiproton collisions in effective Lagrangian and Regge approaches, Eur. Phys. J. A **58**, 32 (2022).
[12] A. T. Goritschnig, P. Kroll, and W. Schweiger, Proton-antiproton annihilation into a $\Lambda_c^+\bar{\Lambda}_c^-$ pair, Eur. Phys. J. A **42**, 43 (2009).
[13] J. Vijande, F. Fernandez, and A. Valcarce, Constituent quark model study of the meson spectra, J. Phys. G **31**, 481 (2005).
[14] J. Segovia, D. R. Entem, F. Fernandez, and E. Hernandez, Constituent quark model description of charmonium phenomenology, Int. J. Mod. Phys. E **22**, 1330026 (2013).
[15] H. Garcilazo, A. Valcarce, and F. Fernandez, Baryon spectrum in the chiral constituent quark model, Phys. Rev. C **63**, 035207 (2001).
[16] J. Vijande, H. Garcilazo, A. Valcarce, and F. Fernandez, Spectroscopy of doubly charmed baryons, Phys. Rev. D **70**, 054022 (2004).
[17] F. Fernández, P. G. Ortega, and D. R. Entem, Quark models of the nucleon-nucleon interaction, Front. Phys. **7**, 233 (2020).
[18] P. G. Ortega, D. R. Entem, and F. Fernandez, Quark model description of the $\Lambda_c(2940)^+$ as a molecular D^*N state and the possible existence of the $\Lambda_b(6248)$, Phys. Lett. B **718**, 1381 (2013).
[19] P. G. Ortega, D. R. Entem, and F. Fernández, LHCb pentaquarks in constituent quark models, Phys. Lett. B **764**, 207 (2017).
[20] D. R. Entem and F. Fernandez, The $N\overline{N}$ interaction in a constituent quark model: Baryonium states and protonium level shifts, Phys. Rev. C **73**, 045214 (2006).
[21] P. Garcia Ortega, D. Rodriguez Entem, and F. Fernández González, Strangeness production in $p\bar{p}$ collision, Hyperfine Interact. **213**, 71 (2012).
[22] A. Manohar and H. Georgi, Chiral quarks and the non-relativistic quark model, Nucl. Phys. **B234**, 189 (1984).
[23] D. Diakonov, Instantons at work, Prog. Part. Nucl. Phys. **51**, 173 (2003).
[24] A. Faessler, G. Lubeck, and K. Shimizu, Nucleon anti-nucleon potential due to the annihilation of one gluon, Phys. Rev. D **26**, 3280 (1982).
[25] E. Hiyama, Y. Kino, and M. Kamimura, Gaussian expansion method for few-body systems, Prog. Part. Nucl. Phys. **51**, 223 (2003).
[26] P. A. Zyla *et al.* (Particle Data Group), Review of particle physics, Prog. Theor. Exp. Phys. **2020**, 083C01 (2020).